CrystEngComm

COMMUNICATION

View Article Online
View Journal | View Issue

Cite this: *CrystEngComm*, 2020, **22**, 2288

Received 17th January 2020,
Accepted 12th March 2020

DOI: 10.1039/d0ce00069h

rsc.li/crystengcomm

Development and characterisation of a cascade of moving baffle oscillatory crystallisers (CMBOC)†

Vishal Raval, Humera Siddique, Cameron J. Brown and Alastair J. Florence *

A novel four stage Cascade of Moving Baffle Oscillatory Crystallisers (CMBOC) is developed, characterised and implemented for continuous crystallisation of pharmaceuticals. The platform was fully automated with pressure controlled slurry transfer and process analytical tools (PAT) to support process monitoring and control. Model predictive control was used to achieve precise temperature control during operation of crystallisations. Mixing and flow characterisation for liquids and slurries was performed confirming near-ideal mixing performance for mean residence times in the range 20–90 min. Heat transfer characteristics were determined and shown to be well suited to the demands of cooling crystallisation processes. Heat transfer efficiency increased with increasing oscillatory Reynolds number (Re_o). This cascade is shown to provide the advantages of more uniform mixing and efficient heat transfer performance compared to a traditional cascade of stirred tank crystallisers. Continuous crystallisations of both alpha lactose monohydrate (ALM) and paracetamol (PCM) were carried out in which the target size, form, agglomeration and encrustation were controlled. For ALM, the products showed a narrow particle size distribution (PSD) with d_v50 = 65 ± 5 μm and a span of 1.4 ± 0.2, and achieved a yield of 70%. The continuous crystallisation of paracetamol in the CMBOC produced non-agglomerated product with d_v50 = 398 ± 20 μm with a span of 1.5 ± 0.2 and achieved an 85% yield. No fouling or encrustation in the vessels or transfer lines were observed during the processes. The flexible configuration and operation of the platform coupled with well characterised shear rate distribution, residence time distributions and heat transfer shows that this platform is well suited to a range of crystallisation modes including seeded, antisolvent, cooling or reactive processes, where careful control of crystal attributes is required.

Strathclyde Institute of Pharmacy & Biomedical Sciences, University of Strathclyde, Technology and Innovation centre, Glasgow, G1 1RD, UK.
E-mail: alastair.florence@strath.ac.uk

† Electronic supplementary information (ESI) available. See DOI: 10.1039/d0ce00069h

Introduction

Continuous manufacturing has attracted considerable attention as an efficient route to convert raw materials into safe, effective and high quality pharmaceutical products.[1,2] In the production of drug substance, the crystallisation process is essential to deliver purity as well as achieving consistent particles with desirable quality attributes including size, shape and form that in turn impact manufacturability, stability and performance. With increasing interest in the industrial adoption of continuous manufacturing, there is a need for robust, well characterised continuous crystallisation process equipment.[1,3] Stirred tank crystallisers (STC) largely remain the standard technology for crystallisation from early stage discovery through to commercial manufacturing. However, they can suffer from batch to batch variability and the need for costly and time consuming scale up to meet increased production demands.[1] However, a number of continuous crystallisers are currently in use in the bulk chemical industry[4] although these have been less applied in the pharmaceutical and fine chemicals sectors due to the scale of operations and the often challenging physical properties of molecular crystals. Therefore, it is not surprising that in the recent years increased research efforts have been made to develop and assess new crystallisers to achieve efficient process operation and enhanced particle control, these include mixed suspension mixed product removal (MSMPR) with single or multiple stages (cascade), plug flow reactors (PFRs) and Couette–Taylor crystallisers.[5–12] Also, well characterised experimental and digital design methodologies for process design, scale-up and optimisation of processes using these technologies have received considerable attention.[13]

MSMPRs remain the most widely utilised platform for continuous crystallisation largely due to familiarity in terms of operation and control to existing batch equipment and these have been successfully operated at a range of scales from 1–10 L.[14] There are however, some recognised disadvantages of

MSMPRs that include localised high shear near the impeller or agitator, non-uniform thermal control and nonlinear process scalability.[15,16] Crystal product quality can be particularly sensitive to the shear rate distribution during crystallisation.[17,18] Chew *et al.*,[18] investigated the shear rate distribution and flow patterns in a stirred tank and in a moving baffle oscillatory crystalliser (MBOC) using computational fluid dynamics (CFD). They showed that in an MBOC, particles spend most of their time in the high shear regions whilst in the STC/MSMPR particles reside mainly in regions of low shear. This has implications on the uniformity of growth, purification, attrition and agglomeration observed in the product.[8,19,20]

PFRs are generally favoured for fast processes with short residence times and can achieve uniform mixing and heat transfer, which is often critical to achieve a well-controlled crystallisation process. For slower processes, such as crystallisation, a very long plug flow crystalliser is usually required to meet the longer residence time requirements and satisfy the flow rates required to achieve plug flow. However, unlike conventional tubular PFR crystallisers, OBCs allow longer residence times to be achieved in a shorter reactor whilst maintaining near plug flow conditions as turbulent mixing is controlled by the oscillatory conditions and decoupled from the net flow rate.[21–27] OBC design principles are described in detail elsewhere.[23] However, they typically comprise of a tubular crystalliser containing periodically spaced annular baffles. Processes are operated by passing a fluid through the crystalliser whilst superimposing an oscillatory motion at the fluid. Oscillatory flow mixing has been developed and investigated as a process intensification technology to achieve efficient and controlled mixing in tubular crystallisers.[28] Whilst OBCs therefore offer a range of favourable characteristics for controlling continuous crystallisation they also present some operating restraints for example poor handling of high solid loadings (typically >20 wt%) and the need to degas the crystalliser to avoid dampening of oscillations.[23,29] Couette–Taylor crystallisers have also received attention for continuous crystallisation. Manipulation of the Taylor vortex flow generated in the gap between two rotating co-axial cylinders has been used to effect control over the crystal size distribution, phase transformation, polymorphic form and agglomeration.[6]

Another important consideration in the design of a crystalliser is its suitability for operating different crystallisation processes including antisolvent, cooling, combined antisolvent-cooling, reactive or pH controlled crystallisations.[15,30] Each crystallisation type requires means of control over particular process parameters. For example, a smooth temperature profile and efficient heat transfer is required in cooling crystallisation (dealing with narrow MSZW processes) and controlled mixing of components is often required for antisolvent and pH controlled crystallisation. Thus for maximum utility, a crystalliser will ideally support different methods of realising supersaturation control *via*: for example flexible addition points for antisolvent or buffers and control of different temperature profiles in addition to offering ease of setup, use and cleaning.[31] Yiging C. Liu *et al.* showed that the MBOC has considerable potential in comparison to a traditional STC to produce narrow product particle size distributions in addition to offering stable and reliable cooling crystallisation operation in a single stage MSMPR in continuous mode.[20] The CMBOC has a number of potential benefits that include handling high solid loadings *via* control of oscillatory conditions. More uniform mixing is achieved compared with a stirred tank by distributing the moving baffles uniformly throughout each vessel.[18,32] Importantly, scale up of this crystalliser setup, as with other oscillatory baffled crystallisers, follows well defined rules maintaining a consistent baffle to orifice ratio and baffle spacing as the size of the reactor changes.[12,23,33]

In this study, a novel four-stage of CMBOC is presented and a detailed characterisation of the mixing and heat transfer performance during continuous operation is reported. The suitability of the system for crystal and particle engineering applications as well as for extended continuous operation at laboratory scale is also investigated for two molecular crystal systems.

Materials and methods

Development of continuous crystallisation platform

The multi vessel cascade of CMBOC consists of four jacketed borosilicate glass vessels with an internal diameter of 25 mm and a height of 220 mm giving a working volume of 120 mL in each vessel. The vessels are mounted on an aluminium frame. A seven-baffle element is present in each vessel to effect mixing. The acetal O-ring baffles have an outer diameter of 24.6 mm, an orifice diameter of 11.2 mm and a thickness of 3 mm giving a tight fit between the moving baffle and inner vessel wall. Baffles were spaced at 37.5 mm using stainless steel spacers. These details were based on the optimal design principles for effective oscillatory mixing reported elsewhere.[25] The oscillatory baffle motion across all the CMBOC stages was provided by means of a linear motor (Copley Controls Corporation) held by an aluminium frame

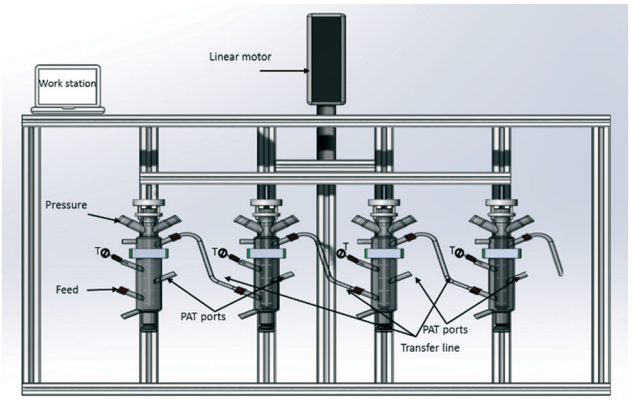

Fig. 1 Schematic showing the CMBOC cascade design.

above the CMBOC (Fig. 1). A control box was used to enable operation of the linear motor over the frequency range of 0–5 Hz and amplitudes of 0–30 mm (peak–peak). Continuous feed transfer between vessels can be done by pressure,[34] vacuum or pump.[20] Pump transfer was deliberately avoided in this setup to minimise any effect on solids due to the mechanical force exerted by the moving parts of the pump. Pressure transfer was implemented by maintaining the CMBOC under positive pressure of 0.02 to 0.05 bar. The benefit of using pressure transfer is that crystals are not exposed to damaging forces and abrupt transfer avoids blockages.[34] Transfer lines between stages were made of jacketed 10 mm I.D. PTFE flexible tubing to minimise heat loss and the risk of uncontrolled fouling during operation. The feed transfer occurs from the top of each stage to the bottom of the next stage to avoid short-circuiting of the fluid between inlet and outlet.[20] There are also two ports available in the middle of each vessel to incorporate PAT probes or for sampling. Both ports are positioned in between two moving baffles. Further ports are positioned at the top of each vessel for additional measurements where required. Each vessel is connected to a bath circulator (Lauda, Eco gold 420) to maintain jacket temperatures. The pumps (Watson Marlow, 520Du) for feed and seed transfer to the first vessel, heater/chiller circulators, pressure regulators, linear motor and thermocouples were interfaced with a PharmaMV control system (Perceptive Engineering Limited, version V7). The PharmaMV Advance Process Control (APC) platform provides an integrated control environment for automation of equipment parameters, collation and archival of process data and the development and operation of real-time model predictive control to automatically control variable process parameters or product attributes.[35]

Results

Flow characterisation

In a continuous flow platform, it is essential to understand the mixing and flow profile achieved under typical operating conditions. The axial dispersion and tanks-in-series models are the most effective methods of estimating residence time distribution (RTD) in a non-ideal platform.[12] These models are widely applied on different types of continuous crystallisers and methods are reported in detail elsewhere.[12,21,36] The experiments were performed by applying the tanks-in-series model over a wide range of oscillatory conditions and net flow rates. A range of oscillatory frequencies (1–3 Hz) and amplitudes (5–20 mm) were investigated with a net flow through the CMBOC cascade ranging from 1–30 mL min^{-1} in order to determine the liquid and solid RTDs. For the liquid RTD study, 3 ml of 0.5 g L^{-1} sodium benzoate tracer were injected into the first vessel. A UV transflectance probe positioned *in situ* in the second and fourth vessel of the CMBOC platform was used to record the absorbance response over time as the tracer elutes.

The dimensionless experimental mean residence time, t_m, and variance of dispersion, σ^2, were calculated against the Re_o which is used here to define the mixing intensity in the CMBOC. Smaller variance values correspond to a more uniform and narrower RTD and are expected to deliver more consistent product. When fluid oscillation is coupled with net flow, σ^2 is affected by three parameters: oscillation frequency, oscillation amplitude and net flowrate.[37] The tanks-in-series model for the liquid RTD was applied for two and four vessel cascade arrangements. Under all the investigated conditions, a good fit was obtained between the experimental data and the theoretical liquid RTD. It also shows a good fit of the theoretical tank-in-series model RTD with experimental conditions, as shown in Fig. 2(A) and S2 in ESI.†

The liquid RTD was assessed for both two and four vessel arrangements. The selection of the number of vessels for a specific process depends on several factors. For example, in crystallisation processes, the number of stages can be finalised based on both supersaturation limits and the required final yield.[10] For both vessel configurations tested here, the experimental mean residence time, t_m, was very close to the theoretical mean residence time, T (see Fig. 2(B)). These results indicate a good overall mixing performance with no significant dead volumes or short-circuiting. For the two vessel arrangement (Fig. 2(C)), σ^2 was higher (average ~0.2) compared to the value obtained for the four vessel arrangement (Fig. 2(D)) (average ~0.1) as expected. Moderate flow rates (5–20 mL min^{-1}) and oscillatory conditions provide less variance as compared to extreme conditions *e.g.* with short-circuiting and dead zones occurring at very high (>25 mL min^{-1}) and very low (<5 mL min^{-1}) flow rates respectively. Also, the addition of more vessels to the cascade changes the flow behaviour towards near plug flow.[33]

Given the aim of assessing, the suitability of the platform to run continuous crystallisations, the mixing and flow performance was also assessed with respect to slurries. To investigate the mean RTD for solids, an FBRM based method was used.[38] For the solid RTD studies, 3 ml of 10 wt% polystyrene particles in water with a d_v50 = 90 μm were injected into the first vessel. FBRM probes positioned in the first and fourth vessel were used to measure the response of the total count of tracer particles passing through the platform over time. The tanks-in-series model provided a reasonable fit between the experimental RTD and theoretical RTD for lower to moderate frequencies and net flowrates (1–2 Hz and 5–20 mL min^{-1}, see Fig. 3(A) and S3 in ESI†). However, a greater deviation from the theoretical RTD was observed at higher frequencies and high net flowrate (3 Hz and 25 mL min^{-1}). This indicates that there is an operating window for effective mixing conditions with slurries based on the current geometry of the platform. Operation outside of this range (<2000 Re_o, >20 mL min^{-1}) will lead to excessive short circuiting and dead zone formation and the system will be no longer be close to an ideal mixing regime.

A similar trend is observed for the mean residence time, t_m, as discussed in the liquid RTD section above (see

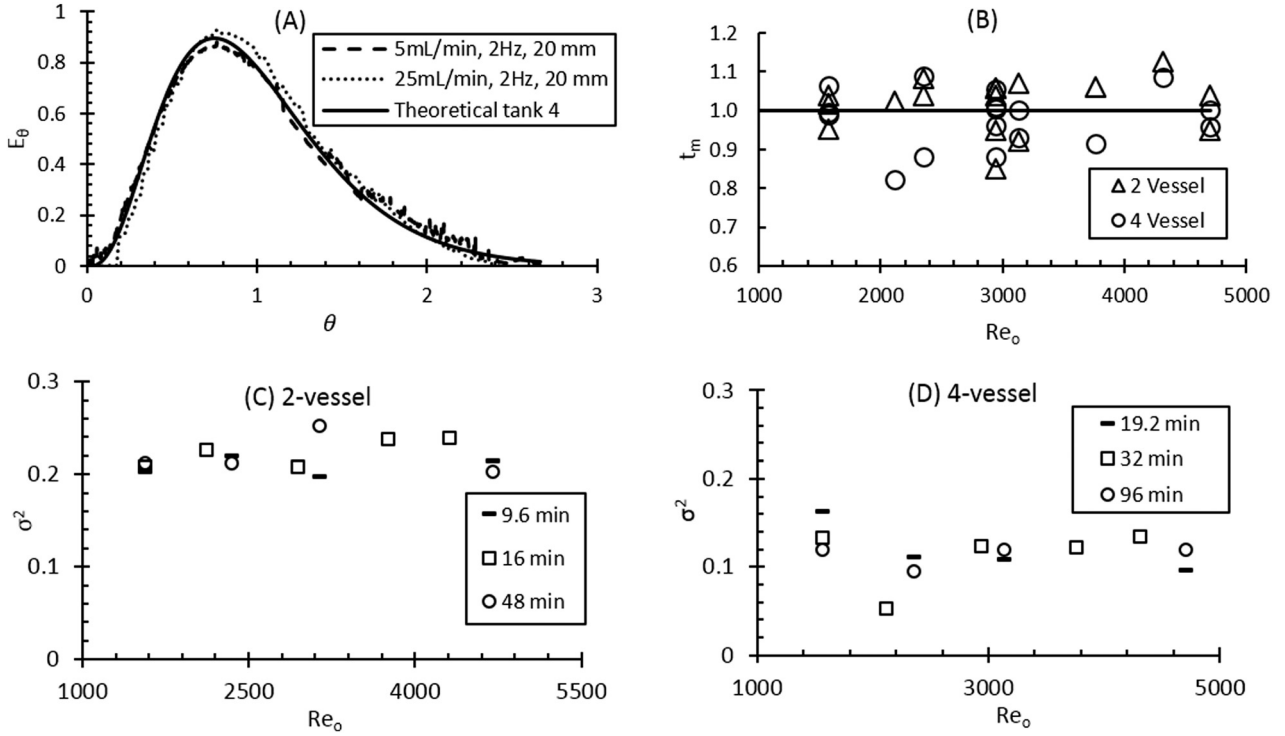

Fig. 2 Liquid RTD study results (A) E_θ *vs.* θ for ALM and PCM operating condition compared with four theoretical tanks-in-series model. (B) Plot of mean residence time, t_m *vs.* Re_O (C) variance of dispersion, σ^2 *vs.* Re_O in 2-vessel cascade (D) variance of dispersion, σ^2 *vs.* Re_O in 4-vessel cascade.

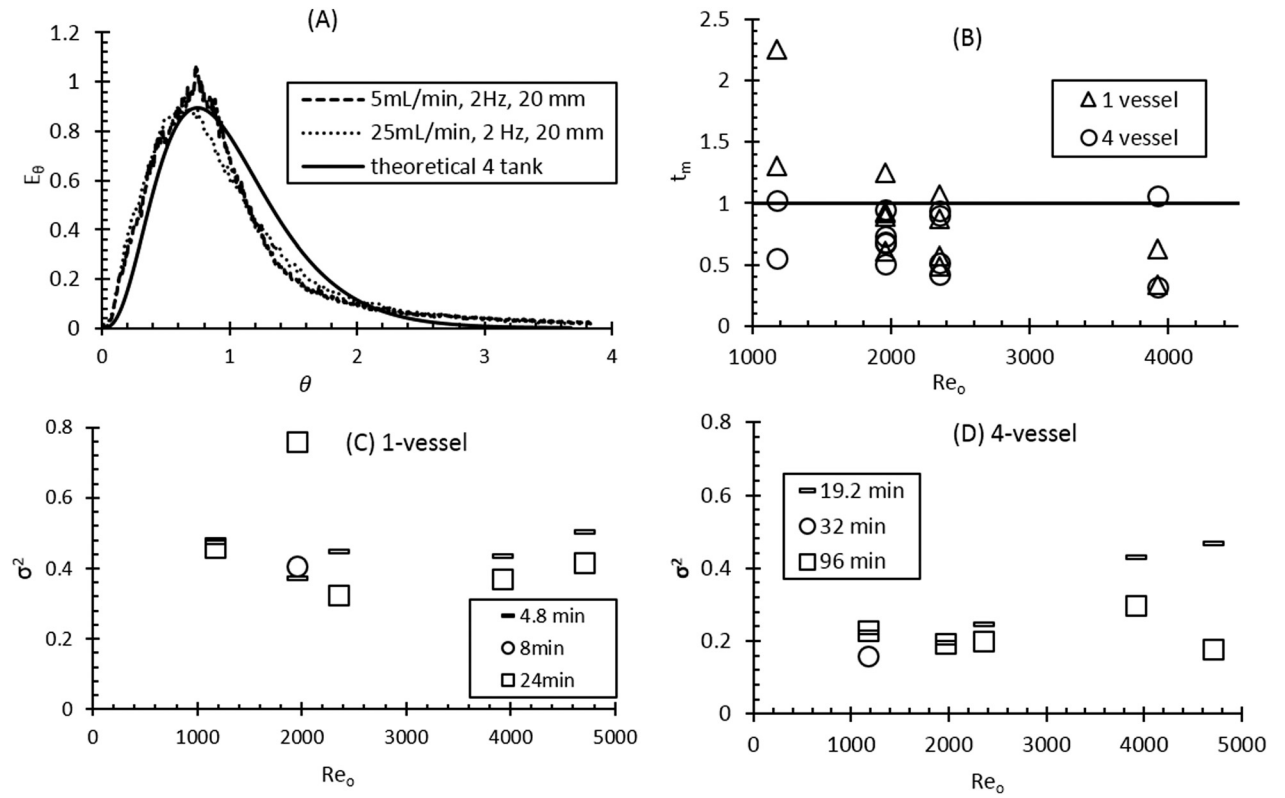

Fig. 3 Solid RTD study results (A) E_θ *vs.* θ for ALM and PCM operating condition with 4 theoretical tanks-in-series model. (B) Plot of mean residence time, t_m *vs.* Re_O (C) variance of dispersion, σ^2 *vs.* Re_O in 1 vessel cascade (D) variance of dispersion, σ^2 *vs.* Re_O in 4 vessel cascade.

Fig. 3(B)). Results related to the increase in variance, σ^2, on moving from one vessel to four vessels were similar to those observed for the liquid RTD. The σ^2 value for solids was almost double that of the liquid only RTD. This is in line

with similar results reported elsewhere for solids RTD.[39,40] This increase in variance is ascribed to the non-Newtonian behaviour of the suspension of particles compared to a solution which is not accounted for in the tanks-in-series model.[39] Another important factor for the increase in variance is the method used for the injection of the tracer pulse. A potential deviation from the model theory is that the slurry pulse was injected over *ca.* 10 s compared to the liquid RTD pulse that was able to be injected near instantaneously. ESI† Table S2 contains further experimental data looking at the specific effects of oscillatory frequency and amplitude on the solid RTD.

Heat transfer characterisation

Heat transfer behaviour was investigated in single stage CMBOC. Heat transfer enhancement due to oscillatory flow by a factor of 10–30 has been reported previously.[41–46] The presence of baffles and oscillatory flow enhances mixing in the radial direction. This radial component ensures rapid fluid movement between the tube wall and the inter baffle region hence improving convective heat transfer.[42] This work focuses on understanding the natural convective heat transfer characteristics under relevant oscillatory conditions for the specific geometry of this platform. The experimental method to characterise this heat transfer performance was adapted from Stephens *et al.*[44] The heat transfer coefficient increased consistently with increasing oscillatory Reynolds number, Re_o (Fig. 4). These results are consistent with previously published data on heat transfer performance of an MBOC.[44] Stephens, *et al.* investigated the heat transfer performance of oscillatory flow crystalliser with fixed baffles and with moving baffle arrangements. A comparison with the heat transfer coefficient in these geometries with that of a stirred tank reactor based on similar power densities concluded that comparable heat transfer coefficients to the STC is achievable in these reactors at very low oscillatory Reynolds numbers.[44] It has been reported that the heat transfer performance of a batch MBOC is similar to a continuous tubular crystalliser operating under turbulent regimes.[44] Adding net flow on top of oscillatory flow further enhances the heat transfer performance. Both CMBOC and tubular crystallisers have higher surface to volume ratios compared to a CSTR making them more efficient in providing uniform heat transfer performance with minimal disturbances.[47,48] The heat transfer characterisation indicates that this system is able to deal effectively with processes where temperature control is crucial for achieving desired product specifications *e.g.* controlled super saturations, heat distribution in exothermic reactions.

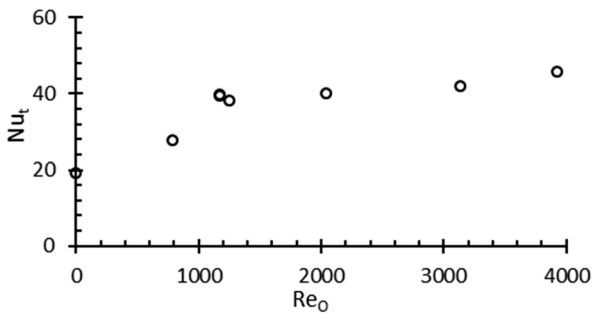

Fig. 4 Effect of oscillatory Reynolds number on the tube side Nusselt number, Nu_t.

Platform assessment for continuous crystallisation

The platform was specifically designed to support the requirements of performing continuous operations such as mixing, synthesis and crystallisation. Having determined the heat transfer characteristics and the liquid and the slurry mixing performance, the CMBOC platform was evaluated by performing continuous crystallisation of two different API's, ALM and PCM that require residence times (RT) of 90 and 20 min respectively.

Continuous cooling crystallisation of alpha lactose monohydrate (ALM)

ALM is widely used as an excipient in pharmaceutical products in particular tablet and inhaled formulations.[49] The crystallisation of lactose has been studied extensively where it can be used to control purity, form control, particle size and shape.[50–54] Industrial challenges include delivering specific particle size distributions to avoid reliance on secondary processes such as sieving and in achieving high product yields. Hence, the aim here was to achieve a narrow particle size distribution span of 1.2–1.6 (for a volume-based size distribution, span = $d_v90 - d_v10/d_v50$) without compromising on yield (target = min 60%). Operating parameters including cooling profile, RT and seed loading for the continuous crystallisation were selected using a lactose crystallisation model. This model was developed from data collected following a sequential parameter estimation approach[55] in a batch MBOC using gPROMS Formulated Product v1.4.0. A 90 min mean RT for a four stage CMBOC was required to achieve the specific target d_v50 = 65 μm with an overall yield of 60%. The target yield was based on the commercially reported yield for ALM.[52,54] Oscillatory conditions were selected based on the RTD results presented above and a frequency of 2 Hz and amplitude of 20 mm were used to minimise axial dispersion at a net flow rate of 4.4 g min^{-1}. The saturated aqueous seed slurry at 50 °C with a d_v50 = 32 μm and a span of 1.1 was introduced continuously at 0.62 g min^{-1} to maintain a seed loading of 1% in the first vessel at a supersaturation of 1.4. The solution concentration and the time for crystallisation to achieve steady state were monitored using an ATR mid-IR probe (ReactIR15) in the second vessel and FBRM in the fourth vessel (trends shown in Fig. S1(A) of ESI†). Steady state was achieved by the end of the third RT and the system was operated for a further 7 RT after steady state. The process start-up from an empty platform involved pumping a saturated aqueous feed solution (46.7

wt%) at 70 °C into the first vessel. Initially temperature control was achieved by controlling all the jacket temperatures at 70 °C and once all the vessels were filled with feed, the temperature in each vessel was controlled using a feedback MPC temperature controller (PharmaMV) with vessel set point temperatures of 55, 44, 37 and 20 °C, for stages 1 to 4 respectively. Product from the final stage was analysed at the end of each RT using laser diffraction, XRPD and microscopy.

The product PSD was consistent from the third RT onwards indicating steady state operation. No signs of fouling or blockages were observed in the transfer lines during the process. Crystals obtained from the CMBOC had a narrow PSD with d_v50 = 65 ± 5 μm and a span of 1.4 ± 0.2 (Fig. 5(A)) and were non-agglomerated with the expected well-defined 'tomahawk' shape.[56,57] (Fig. 6(A)). Crystal form was confirmed using XRPD sample taken from the bulk product and were of the target non-hydrate form (Fig. 7(A)). An overall yield of 70% of ALM was achieved. By comparison commercially available lactose shows a bimodal distribution with a particle span of greater than 2.[54]

Continuous cooling crystallisation of PCM

PCM is widely used as an analgesic and antipyretic and has been studied extensively from a process point of view.[58–60] Extensive work has been carried out on monitoring and production of PCM in batch crystallisers[58] with a few studies conducted on the continuous crystallisation of PCM in both MSMPR and PFR platforms.[60–63] A number of reports have shown fouling problems and blockages of transfer lines during continuous crystallisation of PCM.[59] The aim of this case study was to investigate the feasibility of this platform in performing continuous crystallisation of PCM to deliver form and size control whilst avoiding fouling and agglomeration. This was expected from the uniform mixing and narrow shear distribution in the CMBOC which should lead to less agglomerated product.[39] Crystallisation conditions were selected from preliminary work carried out by Brown, *et al.* for the development of a seeded cooling continuous crystallisation workflow.[13]

PCM crystallisation was performed for five RT where one RT was 20 min. A frequency of 2 Hz and amplitude of 20 mm were used as the oscillatory conditions for effective mixing at the feed flow rate of 18 g min^{-1}. Feed solution concentration of 34.1 wt% solution in 60 : 40 volume of water : isopropanol system. The saturated seed slurry with a d_v50 = 287 μm was introduced continuously in to the first vessel at a flowrate of 5 g min^{-1} with a seed loading of 10 wt% where the temperature was set to achieve a supersaturation of 1.38. The feed vessel was kept at 50 °C and a linear temperature profile was established by maintaining the temperature of four stages at 40, 30, 20 and 10 °C, respectively. Initially temperature control was achieved by controlling all the jacket temperatures at 45 °C and once all the vessels were filled with feed, the temperature in each vessel was controlled using a feedback MPC temperature controller (PharmaMV). Steady state was achieved by the third RT, which was monitored using an inline FBRM probe positioned in vessels 1 and 4 (FBRM trends shown in Fig. S1(B) of ESI†).

The PSD was also consistent by the third RT with a measured d_v50 = 398 ± 20 μm and span of 1.5 ± 0.2 (Fig. 5(B)). The product was non-agglomerated and with well-defined prismatic crystal shapes (Fig. 6(B)). An average thermodynamically achievable yield of 85% was achieved with no evidence of fouling in the vessels and no blockage of the transfer lines observed. The crystals obtained at end of the process were confirmed to be the target form I PCM (Fig. 7(B)). Based on the total RT, the change in median particle size and the achieved yield, an experimentally measured overall average growth rate of 8.90 × 10^{-8} m s^{-1} was estimated. This is comparable to experimentally measured values of 0.67 to 2.56 × 10^{-8} m s^{-1} previously reported in a similar solvent system[64] and are within the range (3.47 to 18.08 × 10^{-8} m s^{-1}) of values estimated for a size dependent growth model.[64]

Operational considerations of the CMBOC

Several operational benefits were identified for the CMBOC based on the two continuous crystallisations performed. The crystallisation start-up procedure, as with other multi-vessel cascade setups, is very efficient as the system can be started by introducing feed and seed flow to the first vessel at time

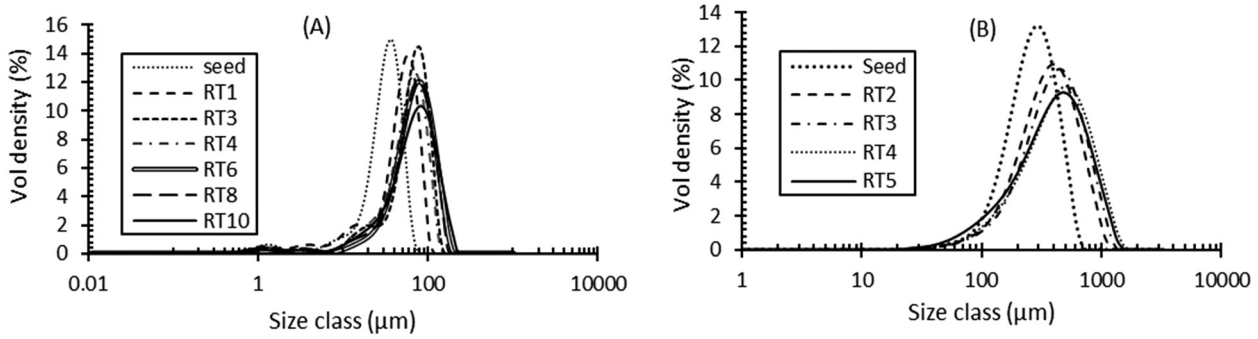

Fig. 5 PSD measurements at successive residence times (RT) for (A) ALM and (B) PCM.

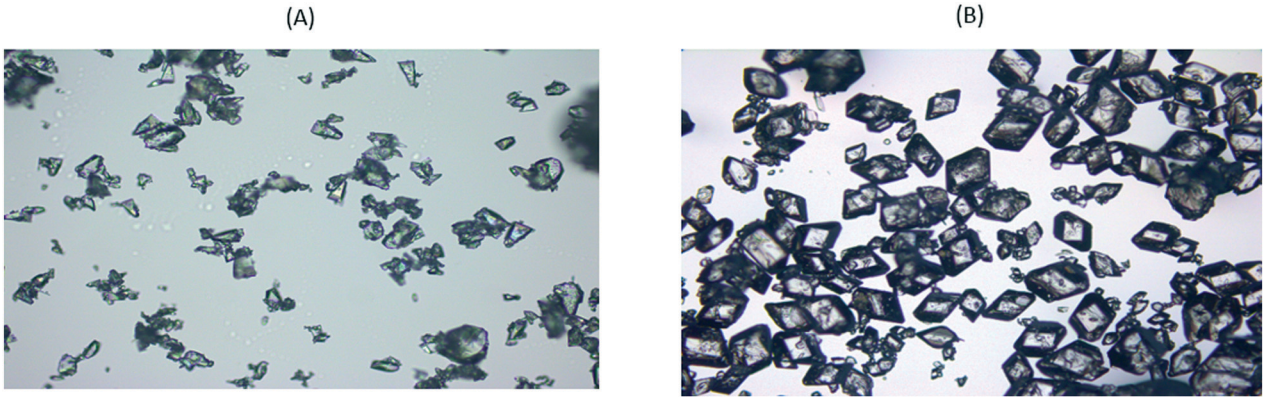

Fig. 6 Microscope images for the products achieved from the CMBOC for (A) ALM and (B) PCM.

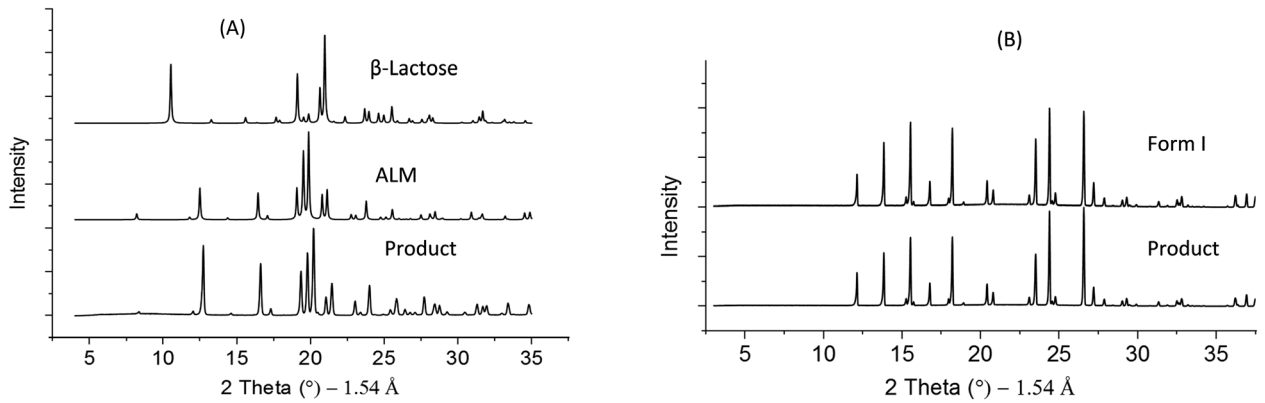

Fig. 7 X-ray powder diffraction patterns for reference forms and bulk product for (A) ALM and (B) PCM.

zero with the entire platform initially empty. The system will reach steady state after third RTs from time zero. Start up with empty vessels is possible in a CSTR assembly but the dead volume is higher in a CSTR compared to a CMBOC before it reaches the mixing point due to the format of the baffle insert. The inlet and outlet points for process streams are designed in such a way to avoid dead volumes and short-circuiting and this is confirmed by the RTD studies. The vessel design also allows for the flexible incorporation of PAT tools and these sensors can be fully integrated to a control system such as PharmaMV to provide closed loop feedback control development and execution.[35,65] Pressure induced slurry transfer between stages was helpful in minimising issues related to transfer line blockages[66] and breakage[13] of crystals that was also as evidenced from the microscopy images of crystals (Fig. 6). The system was able to maintain particle suspension at a solid loading over 30%, significantly greater than is typically achievable for PFRs (~20%).[23,67] In moving fluid oscillatory baffled crystallisers, oscillation dampening is a major issue either due to the presence of gas or the extended length of the crystalliser. The CMBOC therefore offers the advantage of continuous operation without any dampening due to gas or from using an extended number of stages. Longer mean RTs can be easily accommodated by reducing flow rates and/or increasing vessel volume. Further flexibility could be achieved by introducing individual motors to control the oscillation conditions in each vessel which may be beneficial for example in controlling the size of agglomerate in spherical agglomeration processing.[68–70]

Conclusions

This work presents the development of the CMBOC cascade and its characterisation in terms of mixing, heat transfer, solid and liquid flows. The operability and platform performance were assessed by performing two continuous crystallisations for ALM and PCM. The system was run for up to 10 RT in these tests without any operational issues and the target process outcomes in terms of crystal form, particle size and yield were achieved consistently. The key actuator and sensor components of this novel crystalliser platform have been automated with data stream integrated using a PharmaMV control system to ease setup of equipment and ancillaries (heater chillers and linear motor pumps and pressure controller) for process start up and to precisely control all the operating parameters in the crystalliser during operation.

For a broad range of conditions, experimental RTD were found to be consistent with theoretical RTD from a tanks-in-series model, showing efficient and well-mixed mixing performance. This predictable performance, allows for ease of process design. The system was also characterised for heat

transfer performance and it was revealed that the oscillatory conditions have a major contribution towards the enhanced heat transfer performance of the platform. It can be concluded from the outcomes of the crystallisation operations that this platform has the capability to deal with several challenges related to continuous crystallisation such as fouling and operating at higher solid loadings. An additional benefit of this platform includes the ability to achieve narrow PSDs and lower agglomeration. No evidence of significant attrition was observed during these studies.

Future work will focus on coupling continuous primary nucleation using sonication, wet milling and operation beyond MSZW in the first vessel with controlled growth for both cooling and antisolvent crystallisation processes. The robust and controllable performance of this system shows potential as a flexible, adaptable microfactory module capable of producing up to several kg per day. This can have direct application during early stage development for access to different grades of materials, as well as for small scale manufacturing where consistently high quality product is required.

Nomenclature

CMBOC	Cascade of moving baffle oscillatory crystallisers
MBOC	Moving baffle oscillatory crystallisers
OBC	Oscillatory baffle crystalliser
MSZW	Meta stable zone width
τ	Theoretical mean residence time
t_m	Dimensionless experimental mean residence time
$\bar{t}$	Experimental mean residence time
θ	Dimensionless time based on the mean residence time in all tank
σ^2	Variance or a measure of the spread of the curve
C_i	Concentration of tracer at i time interval
Δt	Difference between each time interval
E_θ	Exit age distribution function
N	Number of tanks
ω	Oscillation frequency
x_0	Oscillation amplitude
D	Diameter of vessel
μ	Viscosity of fluid
ρ	Density of fluid
Re_o	Oscillatory Reynolds number = $(2\pi\omega x_0\rho D)/\mu$
Nu_t	Tube side Nusselt number
d_v10	Size point below which 10% of the material is contained
d_v50	Size point below which 50% of the material is contained
d_v90	Size point below which 90% of the material is contained

Conflicts of interest

There are no conflicts to declare.

Acknowledgements

The authors are grateful to the University of Strathclyde for funding Vishal Raval's studentship and to EPSRC, Future Continuous Manufacturing and Advanced Crystallisation Research Hub (Grant Ref EP/P006965/1) for funding. The authors also acknowledge support for the CMAC National Facility from the UK Research Partnership Infrastructure Fund award from the Higher Education Funding Council for England (HEFCE; Grant Ref HH13054). The authors also thank Ali Anwar for support for the CAD design.

References

1 I. R. Baxendale, R. D. Braatz, B. K. Hodnett, K. F. Jensen, M. D. Johnson, P. Sharratt, J.-P. Sherlock and A. J. Florence, *J. Pharm. Sci.*, 2015, **104**, 781–791.
2 T. Page, H. Dubina, G. Fillipi, R. Guidat, S. Patnaik, P. Poechlauer, P. Shering, M. Guinn, P. McDonnell and C. Johnston, *J. Pharm. Sci.*, 2015, **104**, 821–831.
3 J. C. McWilliams, A. D. Allian, S. M. Opalka, S. A. May, M. Journet and T. M. Braden, *Org. Process Res. Dev.*, 2018, **22**, 1143–1166.
4 F. Ref, FLUENT 5.
5 A.-T. Nguyen and W.-S. Kim, *Korean J. Chem. Eng.*, 2017, **34**, 1896–1904.
6 S. Lee, C.-H. Lee and W.-S. Kim, *J. Cryst. Growth*, 2017, **469**, 119–127.
7 Q. Khuu, G. Dang, H. Trinh and T. Nguyen, *Science and Technology Development Journal*, 2016, **19**, 11–23.
8 S. Lawton, G. Steele, P. Shering, L. H. Zhao, I. Laird and X. W. Ni, *Org. Process Res. Dev.*, 2009, **13**, 1357–1363.
9 P. Neugebauer and J. G. Khinast, *Cryst. Growth Des.*, 2015, **15**, 1089–1095.
10 Q. Su, Z. K. Nagy and C. D. Rielly, *Chem. Eng. Process.: Process Intesif.*, 2015, **89**, 41–53.
11 N. S. Tavare, *AIChE J.*, 1986, **32**, 705–732.
12 O. Levenspiel, *Chemical Reaction Engineering*, John Wiley & Sons, New York Chichester Weinheim Brisbane Singapore Toronto, 3rd edn, 1962.
13 C. J. Brown, T. McGlone, S. Yerdelen, V. Srirambhatla, F. Mabbott, R. Gurung, M. L. Briuglia, B. Ahmed, H. Polyzois, J. McGinty, F. Perciballi, D. Fysikopoulos, P. MacFhionnghaile, H. Siddique, V. Raval, T. S. Harrington, A. D. Vassileiou, M. Robertson, E. Prasad, A. Johnston, B. Johnston, A. Nordon, J. S. Srai, G. Halbert, J. H. ter Horst, C. J. Price, C. D. Rielly, J. Sefcik and A. J. Florence, *Mol. Syst. Des. Eng.*, 2018, **3**, 518–549.
14 S. Mascia, P. L. Heider, H. T. Zhang, R. Lakerveld, B. Benyahia, P. I. Barton, R. D. Braatz, C. L. Cooney, J. M. B. Evans, T. F. Jamison, K. F. Jensen, A. S. Myerson and B. L. Trout, *Angew. Chem., Int. Ed.*, 2013, **52**, 12359–12363.
15 J. Chen, B. Sarma, J. M. B. Evans and A. S. Myerson, *Cryst. Growth Des.*, 2011, **11**, 887–895.
16 K. Plumb, *Chem. Eng. Res. Des.*, 2005, **83**, 730–738.
17 C. M. Chew and R. I. Ristic, *AIChE J.*, 2005, **51**, 1576–1579.

18 C. M. Chew, R. I. Ristic, G. K. Reynolds and R. C. Ooi, *Chem. Eng. Sci.*, 2004, **59**, 1557–1568.
19 R. I. Ristic, *Chem. Eng. Res. Des.*, 2007, **85**, 937–944.
20 Y. Q. C. Liu, D. Dunn, M. Lipari, A. Barton, P. Firth, J. Speed, D. Wood and Z. K. Nagy, *Chem. Eng. J.*, 2019, **367**, 278–294.
21 P. Stonestreet and P. M. J. Van der Veeken, *Chem. Eng. Res. Des.*, 1999, **77**, 671–684.
22 A. W. Dickens, M. R. Mackley and H. R. Williams, *Chem. Eng. Sci.*, 1989, **44**, 1471–1479.
23 T. McGlone, N. E. B. Briggs, C. A. Clark, C. J. Brown, J. Sefcik and A. J. Florence, *Org. Process Res. Dev.*, 2015, **19**, 1186–1202.
24 T. Howes and M. R. Mackley, *Chem. Eng. Sci.*, 1990, **45**, 1349–1358.
25 X. W. Ni, *J. Chem. Technol. Biotechnol.*, 1995, **64**, 165–174.
26 K. B. Smith and M. R. Mackley, *Chem. Eng. Res. Des.*, 2006, **84**, 1001–1011.
27 N. E. B. Briggs, U. Schacht, V. Raval, T. McGlone, J. Sefcik and A. J. Florence, *Org. Process Res. Dev.*, 2015, **19**, 1903–1911.
28 A. P. Harvey, M. R. Mackley and T. Seliger, *J. Chem. Technol. Biotechnol.*, 2003, **78**, 338–341.
29 B. J. Doyle, B. Gutmann, M. Bittel, T. Hubler, A. Macchi and D. M. Roberge, *Ind. Eng. Chem. Res.*, 2019, **59**, 4007–4019.
30 M. Jiang and X.-W. Ni, *Org. Process Res. Dev.*, 2019, **23**, 882–890.
31 C. Ricardo and N. Xiongwei, *Org. Process Res. Dev.*, 2009, **13**, 1080–1087.
32 M. H. I. Baird, N. V. Rama Rao, J. Prochazka and H. Sovova, *Reciprocating plate columns in solvent extraction equipment design*, Wiley, Chichester UK, 1994.
33 O. Levenspiel, *Chemical Reaction Engineering*, Wiley, New York, USA, 3rd edn, 1999.
34 Y. Cui, M. O'Mahony, J. J. Jaramillo, T. Stelzer and A. S. Myerson, *Org. Process Res. Dev.*, 2016, **20**, 1276–1282.
35 F. Tahir, K. Krzemieniewska-Nandwani, J. Mack, D. Lovett, H. Siddique, F. Mabbott, V. Raval, I. Houson and A. Florence, *Control Eng. Pract.*, 2017, **67**, 64–75.
36 P. Cruz, C. Silva, F. Rocha and A. Ferreira, *AIChE J.*, 2019, **65**, e16683.
37 M. Z. Zheng and M. Mackley, *Chem. Eng. Sci.*, 2008, **63**, 1788–1799.
38 R. Kacker, S. I. Regensburg and H. J. M. Kramer, *Chem. Eng. J.*, 2017, **317**, 413–423.
39 M. Manninen, E. Gorshkova, K. Immonen and X. W. Ni, *J. Chem. Technol. Biotechnol.*, 2013, **88**, 553–562.
40 I. I. Onyemelukwe, Z. K. Nagy and C. D. Rielly, *Chem. Eng. J.*, 2019, 122862.
41 M. R. Mackley, G. M. Tweddle and I. D. Wyatt, *Chem. Eng. Sci.*, 1990, **45**, 1237–1242.
42 M. R. Mackley and P. Stonestreet, *Chem. Eng. Sci.*, 1995, **50**, 2211–2224.
43 Z. D. Chen and J. J. J. Chen, *Chem. Eng. Sci.*, 1998, **53**, 3177–3180.
44 G. G. Stephens and M. R. Mackley, *Exp. Therm. Fluid Sci.*, 2002, **25**, 583–594.
45 X. R. Zhang, S. Maruyama and S. Sakai, *Int. J. Heat Mass Transfer*, 2004, **47**, 4439–4448.
46 E. M. Benavides, *J. Appl. Phys.*, 2009, **105**, 094907.
47 M. Danish, M. Al Mesfer, M. Md and M. Rashid, *Int. J. Eng. Res. Ind. Appl.*, 2015, **5**, 2248–962274.
48 M. A. Javinsky, *AIChE J.*, 1970, 916–924.
49 P. L. H. McSweeney and P. F. Fox, *Advanced Dairy Chemistry, Lactose, Water, Salts and Minor Constituents*, Springer-Verlag, New York, 2009.
50 S. Y. Wong, R. K. Bund, R. K. Connelly and R. W. Hartel, *Cryst. Growth Des.*, 2010, **10**, 2620–2628.
51 S. Y. Wong, R. K. Bund, R. K. Connelly and R. W. Hartel, *Int. Dairy J.*, 2011, **21**, 839–847.
52 S. Y. Wong and R. W. Hartel, *J. Food Sci.*, 2014, **79**, R257–R272.
53 S. Y. Wong, A. P. Tatusko, B. L. Trout and A. S. Myerson, *Cryst. Growth Des.*, 2012, **12**, 5701–5707.
54 J. Mcleod, *doctor of Philosophy*, Massey University, 2007.
55 J.-F. Pérez-Calvo, S. S. Kadam and H. J. M. Kramer, *AIChE J.*, 2016, **62**, 3992–4012.
56 Y. Shi, B. Liang and R. W. Hartel, *J. Food Sci.*, 1990, **55**, 817–820.
57 B. Liang, Y. Shi and R. W. Hartel, *J. Food Sci.*, 1991, **56**, 848–854.
58 M. Fujiwara, P. S. Chow, D. L. Ma and R. D. Braatz, *Cryst. Growth Des.*, 2002, **2**, 363–370.
59 K. A. Powell, A. N. Saleemi, C. D. Rielly and Z. K. Nagy, *Chem. Eng. Process.: Process Intesif.*, 2015, 195–212.
60 C. J. Brown and X. W. Ni, *Cryst. Growth Des.*, 2011, **11**, 3994–4000.
61 C. M. Chew, R. I. Ristic, R. D. Dennehy and J. J. De Yoreo, *Cryst. Growth Des.*, 2004, **4**, 1045–1052.
62 C. J. Brown and X. W. Ni, *Cryst. Growth Des.*, 2011, **11**, 719–725.
63 H. G. Jolliffe and D. I. Gerogiorgis, *Comput. Chem. Eng.*, 2018, **118**, 224–235.
64 G. Hou, G. Power, M. Barrett, B. Glennon, G. Morris and Y. Zhao, *Cryst. Growth Des.*, 2014, **14**, 1782–1793.
65 H. Siddique, C. J. Brown, I. Houson and A. J. Florence, *Org. Process Res. Dev.*, 2015, **19**, 1871–1881.
66 I. I. Onyemelukwe, A. R. Parsons, H. P. Wheatcroft, A. Robertson, Z. K. Nagy and C. D. Rielly, *Cryst. Growth Des.*, 2019, **19**, 66–80.
67 L. Zhao, V. Raval, N. E. B. Briggs, R. M. Bhardwaj, T. McGlone, I. D. H. Oswald and A. J. Florence, *CrystEngComm*, 2014, **16**, 5769–5780.
68 R. Peña and Z. K. Nagy, *Cryst. Growth Des.*, 2015, **15**, 4225–4236.
69 P. M. Orlewski, B. Ahn and M. Mazzotti, *Cryst. Growth Des.*, 2018, **18**, 6257–6265.
70 K. Pitt, R. Peña, J. D. Tew, K. Pal, R. Smith, Z. K. Nagy and J. D. Litster, *Powder Technol.*, 2018, **326**, 327–343.

